Capturing the Abnormal Brain Network Activity in Early Parkinsons Disease With Mild Cognitive Impairment Based on Dynamic Functional Connectivity

Guosheng Yi, Yanbo Wang, Liufang Wang, Chunguang Chu, Jiang Wang, *Member, IEEE*, Xiao Shen, Xiaoxuan Han, Zhen Li, Lipeng Bai, Zhuo Li, Rui Zhang, Yanlin Wang, Xiaodong Zhu, and Chen Liu, *Member, IEEE*

***Abstract*— The early Parkinson's disease (PD) with mild cognitive impairment (ePD-MCI) is a typical non-motor symptom reflected by the brain dysfunction of PD, which can be well depicted by the dynamic characteristics of brain functional connectivity networks. The aim of this study is to determine the unclear dynamic changes in functional connectivity networks induced by MCI in early PD patients. In this paper, the electroencephalogram (EEG) of each subject was reconstructed into the dynamic functional connectivity networks with five frequency bands based on adaptive sliding window method. By evaluating the fluctuations of dynamic functional connectivity and the transition stability of functional network state in ePD-MCI patients compared with early PD without mild cognitive impairment patients, it was found that in the alpha band, the functional network stability of central region, right frontal, parietal, occipital, and left temporal lobes was abnormally increased, and the dynamic connectivity fluctuations in these regions were significantly decreased in ePD-MCI group. In the gamma band, ePD-MCI patients showed decreased functional network stability in the central, left frontal, and right temporal lobes, and active dynamic connectivity fluctuations in the left frontal, temporal, and parietal lobes. The aberrant duration of network state in ePD-MCI patients was significantly negatively correlated with cognitive function in the alpha band, which might pave the way to identify and predict cognitive impairment in early PD patients.**

***Index Terms*— Parkinson's disease, mild cognitive impairment, brain functional connectivity, network state transition.**

Manuscript received 16 December 2021; revised 27 August 2022, 5 October 2022, and 11 January 2023; accepted 30 January 2023. Date of publication 6 February 2023; date of current version 14 February 2023. This work was supported in part by the Natural Science Foundation of Tianjin, China, under Grant 20JCQNJC01160, Grant 19JCQNJC01200, and Grant 18JCZDJC32000; in part by the Foundation of Tianjin University under Grant 2020XRG-0018; in part by the Opening Foundation of Key Laboratory of Opto-Technology and Intelligent Control (Lanzhou Jiaotong University), Ministry of Education, under Grant KFKT2020-01; in part by the Tianjin Health Commission under Grant TJWJ2022MS004 and Grant 2023001; and in part by the Tianjin Municipal Science and Technology Commission under Grant 22YDTPJC00350. *(Corresponding authors: Chunguang Chu; Xiaodong Zhu; Chen Liu.)*

Guosheng Yi, Yanbo Wang, Liufang Wang, Chunguang Chu, Jiang Wang, and Chen Liu are with the School of Electrical and Information Engineering, Tianjin University, Tianjin 300072, China (e-mail: ccg_tina@tju.edu.cn; liuchen715@tju.edu.cn).

Xiao Shen, Zhen Li, Zhuo Li, Rui Zhang, Yanlin Wang, and Xiaodong Zhu are with the Department of Neurology, Tianjin Medical University General Hospital, Tianjin 300052, China (e-mail: zxd3516@tmu.edu.cn).

Xiaoxuan Han and Lipeng Bai are with the Department of Neurology, Tianjin Neurological Institute, Tianjin Medical University General Hospital, Tianjin 300052, China.

This article has supplementary downloadable material available at https://doi.org/10.1109/TNSRE.2023.3243035, provided by the authors.

Digital Object Identifier 10.1109/TNSRE.2023.3243035

I. Introduction

PARKINSON's disease (PD) a neurodegenerative disease in the central nervous system [1], whose clinical manifestations included motor symptoms (bradykinesia, rigidity, resting tremor, etc.) and non-motor symptoms [2]. About a quarter of PD patients are diagnosed to be accompanied with mild cognitive impairment (MCI) [3]. And cognitive impairment greatly increases the risk of developing dementia in PD as it progresses [4]. Symptoms such as planning impairment, intellectual disability, and memory impairment caused by Parkinson's disease dementia (PDD) will seriously harm patients' health [5]. Thus, in order to prevent the occurrence of PDD more effectively, early research of Parkinson's disease with mild cognitive impairment (PD-MCI) is necessary.

Abnormal local electrical activity in the brain of early PD patients can be detected and recorded by electroencephalogram (EEG) [6]. It has been shown that Parkinson's patients have abnormal changes in certain frequency bands of EEG [7]. Chaturvedi et al. [8] used phase lag index (PLI) to identify patients with early PD-MCI based on EEG, and the identification effect was related to EEG frequency bands. Bousleiman et al. [9] found that patients with PD-MCI had reduced alpha-band power compared with patients with normal PD. Therefore, in this study, we analyzed the abnormal brain dynamic activities of patients in five bands (delta, theta, alpha, beta, and gamma) of EEG.

In PD-MCI patients, structural networks of basal ganglia and frontotemporal-parietal lobe were found to be disrupted based on a functional Magnetic Resonance Imaging (fMRI) analysis, and the change of the network may be associated with functional connectivity structural disturbances in PD-MCI patients [10]. In addition, Bezdicek et al. [11] also confirmed that cognitive impairment may lead to disruption of brain connectivity by observing reduced bilateral parietal and precuneus connectivity in PD-MCI patients. Considering early Parkinson's disease with mild cognitive impairment (ePD-MCI) is a typical non-motor symptom reflected by dysfunction of brain network, graph theory can characterize the interrelated structures of the patients brain to understand the related brain networks [12]. Based on graph theory, Chaturvedi et al. [8] found that the PLI had better effect than frequency measurement, and Suarez et al. [13] found that PD-MCI patients had reduced functional connectivity in the alpha and delta bands. The static functional connectivity which is used frequently assumes that statistical dependencies between different brain regions remain stable over time in the resting state [14]. However, the inside of the brain is active and organized, albeit in the resting state [15], [16]. The dynamic functional network represents the non-stationary patterns of brain state during the temporal evolution of brain function, describing the topology of the network on spatial scale and the dynamic fluctuation on temporal scale [17]. Hence, dynamic functional connectivity (dFC) is worthing to be explored. To this end, we investigated the dFC patterns of ePD-MCI on the millisecond timescale. Based on dFC, Diez-Cirarda et al. [18] found that PD-MCI patients had an increased number of state transitions in low functional connectivity state and network instability state compared with healthy control (HC). Therefore, some dynamic network parameters reflecting the state transition of brain network can be used as biomarkers to judge PD-MCI patients. In this work, we used transitional stability to characterize brain dynamic functional networks (DFNs) and to find abnormal changes in different regions of the brain in patients with ePD-MCI.

MCI is more common in early PD. In the middle and late stages of PD, cognitive impairment often develops into dementia with temporal evolution. Thus, to investigate the effect of MCI in PD on the temporal evolution of DFNs in the brain, this work aims to understand the differences in brain activity underlying ePD-MCI symptoms and to obtain the potential biomarker of ePD-MCI by analyzing abnormal fluctuations of brain functional connectivity and network state transitions associated with ePD-MCI. Further combining the results with clinical neuropathological scores to pave the way to identify and predict cognitive impairment in early PD patients.

II. Materials and Methods

A. Subjects

In our work, 33 patients with primary PD and 13 HC were recruited from Tianjin Medical University General Hospital. All patients had early PD with Hoehn and Yahr (H&Y) stage I-II. All patients were asked to interrupt their medication 12 hours before collecting the EEG signals to rule out any effect of medication on the results. All patients ensured no head tremors when collecting EEG to exclude interference. Patients with cerebrovascular disease and cognitive impairment within two years of PD diagnosis were excluded. All patients took part in cognitive function tests. According to the Montreal Cognitive Assessment (MoCA) scale, the score between 21 and 25 was defined as MCI, and the score between 26 and 30 was defined as cognitively normal. According to this criterion, PD patients were divided into two groups: 13 patients with ePD-MCI and 20 patients with early Parkinson's disease without mild cognitive impairment (ePD-nMCI). Table I recorded the basic information of subjects in the three groups. The differences between ePD-MCI and ePD-nMCI patients were analyzed by ANOVA method. And the only significant difference between the two groups was on the MOCA scale. The local ethics committee approved the work, and the work obtained informed consent from the subjects, which was in accordance with the Helsinki Declaration.

TABLE I
Basic Information of Participants

	ePD-MCI (n=13)	ePD-nMCI (n=20)	Healthy Controls (n=13)	ePD-MCI vs. ePD-nMCI
	mean (S.D.)	mean (S.D.)	mean (S.D.)	p-value
Age	62.00 (8.35)	63.50 (6.30)	62.54(5.01)	n.s.
H-Y stage	1.50 (0.58)	1.18 (0.44)	n.a.	n.s.
Course of the disease	3.38 (2.72)	4.58 (4.50)	n.a.	n.s.
MoCA scale	23.00 (1.83)	27.70 (1.30)	n.a.	$p < 0.01$
RBDSQ	0.54 (1.66)	0.55 (1.64)	n.a.	n.s.

S.D. = Standard Deviation; n.a. = not applicable; n.s. = no significance.

B. EEG Acquisition and Preprocessing

The EEG acquisition equipment in this experiment was an amplifier (Symtop, Beijing, China) and the silver chloride powder electrode cap. The sampling frequency of the amplifier was 500Hz. According to the international 10-20 system of Electrode, a total of 19 EEG signals were collected. In addition, four additional signal channels (above and below the eyes, left and right temples) were collected to record horizontal and vertical electrooculogram (EOG) respectively, which were used to monitor the eye movement and blinking of subjects during the collection process, so as to remove ocular artifacts during preprocessing. The subjects were asked to lie flat in a quiet and dim room, close their eyes and stay awake. And then they wore an electrode cap to collect resting EEG signals. The EEG collection time of each subject was more than 15 minutes.

The collected EEG signals were preprocessed with MATLAB 2018b (MathWorks Inc., Natick MA, United States). The collected scalp brain electrical signals had high-frequency interference of equipment noise, so it was necessary to filter out the noise. The zero-phase shift filtering that does not change the phase relationship of EEG data was used to determine the spectral range from 1 to 45Hz [19]. In the work, fastICA (fast Independent Component Analysis) algorithm was used to extract the relevant independent components from the 19-channel EEG signals, and the pearson correlation

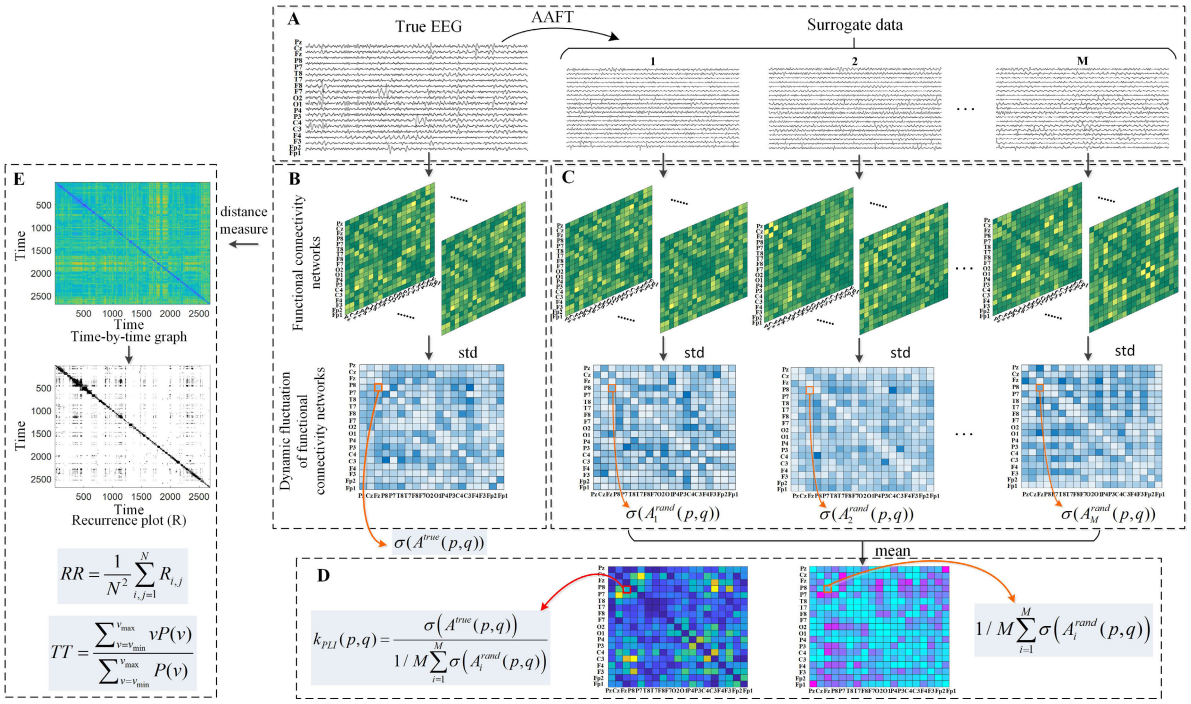

Fig. 1. Fluctuation analysis of the dFC. (A) The surrogate data produced by AAFT. (B)-(C) DFNs were created using several *PLI* windows based on authentic EEG and surrogate data. By analyzing the standard deviation of *PLI* sequence between *p* and *q* channels in each time window, the dynamic changes of brain connectivity between the respective channels were determined. (D) Calculating the ratio of the standard deviation of the real data and the standard deviation of the surrogate data to obtain the real fluctuation of the brain dynamic functional connectivity, which denotes as k_{PLI}. (E) Network state transition analysis.

coefficient was used to calculate the correlation between each component and the horizontal and vertical EOG [20]. The component with the absolute value of correlation coefficient greater than 0.5 was considered to have strong correlation with the collected EOG, and the component strongly correlated with EOG was set to zero and filtered out. Finally, the large noise interference which was difficult to be eliminated by the algorithm was removed by artificial eyes. The preprocessed EEG signals were divided into five frequency bands by zero-phase shift filtering, which were delta band (1-4Hz), theta band (4-8Hz), alpha band (8-13Hz), beta band (13-30Hz), and gamma band (30-45Hz) [21]. And we analyzed the characteristics of dynamic brain functional network based on the five sub-bands.

C. Construction of the DFNs Based on Adaptive Sliding Window

In this paper, an adaptive sliding-window method based on empirical mode decomposition (EMD) was used to estimate the local stationary process of dynamic brain activity in patients. The EMD method has an effective ability to characterize the local transient feature of time-varying nonlinear and non-stationary signals. Moreover, the sliding window extracted by EMD is adaptively determined according to the data. The DFNs constructed by different individuals are different, which is more helpful to capture information with significant differences in the time-varying process [22]. Time-dependent sliding-windows are determined based on the frequency content of each time point of the data itself without any prior information. The research has proved that the single-scale time-dependent window size captures the time-related period (reciprocal of frequency) information at each time point, and the results showed that this adaptive window method can capture more dynamic information related to behavioral and cognitive functions. The definition of EMD and the calculation method of time-dependent windows were given in the supplementary material. Zhuang et al. [23] have demonstrated the effectiveness of this method. Based on the adaptive sliding-window method, the process of constructing DFNs was from Fig. 1A to B. And the number and lengths of windows divided by the data in this paper were described in Tables I and II of the supplementary material.

Then, we constructed the DFNs through PLI based on adaptive sliding window. PLI was proposed by Stam et al. [24], whose main purpose is to obtain reliable estimates of phase synchronization. PLI is used to calculate the degree of phase coupling between two time series, which is obtained by calculating the instantaneous phase of the EEG signal and the asymmetry of the phase difference distribution between the two signals. The formula is shown below

$$PLI = |\langle \mathrm{sign}\left[\Delta\phi\left(t_k\right)\right]\rangle|, \quad k = 1, 2, \ldots, N \tag{1}$$

where $\Delta\phi\left(t_k\right)$ is the time series of phase differences calculated at N time points. The range of PLI is from 0 to 1. With the increase of PLI, the coupling strength between signals increases gradually. $PLI = 0$ indicates no phase difference or no coupling centered around 0 mod π and $PLI = 1$ means a perfect phase locking around 0 mod π. And we obtained DFNs for each subject, which was a PLI matrix of 19*19*N, where N was the number of windows.

D. Fluctuation Analysis of the dFC

The diagram of fluctuation analysis of the dFC was shown in Fig. 1A-D.

By calculating the standard deviation of PLI sequence between channels in each time window throughout the dynamic process of DFNs, the dynamic fluctuation characteristics of brain connectivity between corresponding channels were characterized. However, the noise of EEG signals was likely to cause random fluctuations in functional connectivity. Therefore, when analyzing the fluctuations of dFC in ePD-MCI patients and ePD-nMCI patients, the fluctuations of functional connectivity based on the true EEG signals of subjects were not enough to prove the existence of dFC. In order to observe whether the fluctuation of functional connectivity can reflect the real dFC, surrogate data was introduced to solve this problem (see Fig. 1A). We evaluated the authenticity of fluctuations by selecting an appropriate zero model to represent a stationary process. Based on the surrogate data under the same sliding window, a functional network was established to calculate the dynamic fluctuation of the functional connectivity of the surrogate data. In this paper, the amplitude adjusted Fourier transform (AAFT) was chosen to construct zero model [25]. The AAFT method was used to generate 20 sets of surrogate data corresponding to the true EEG, and the corresponding surrogate data was divided according to the sliding-window determined by the corresponding true EEG sequence, and the DFNs based on PLI were also constructed. The surrogate data also calculated dynamic fluctuation characteristics in the same way as the true EEG and the mean fluctuation of 20 groups of surrogate data was calculated (see Fig. 1B and C). Then we calculated the ratio of the standard deviation of the real data and the standard deviation of the surrogate data, denoted as k_{PLI} shown in Fig. 1D. k_{PLI} is given by

$$k_{PLI}(p,q) = \frac{\sigma\left(A^{\text{true}}(p,q)\right)}{1/M\sum_{i=1}^{M}\sigma\left(A_i^{\text{rand}}(p,q)\right)} \tag{2}$$

where A represents the DFNs which is PLI matrix of 19*19*number of windows, p and q are the indexes of EEG channels, and M is the group number of surrogate data generated. The k_{PLI} of p channel is the average of the column with p as the abscissa. And the whole brain k_{PLI} is the average of all channels. The k_{PLI} compares fluctuations of true data with fluctuations of random data, which can be used to see if there are real fluctuations in dynamic brain functional connectivity. The larger the value is, the stronger the dynamic fluctuation of functional connectivity is.

E. Network State Transition Analysis

The diagram of network state transition analysis was shown in Fig. 1E.

1) Time-by-Time Graph: In the process of constructing the time-by-time graph [26], we defined time in the form of PLI sequences in DFNs. The edges of the time-by-time graph represented the DFNs time points, while the points on the graph represented the similarity between the associated DFNs at various time points. The similarity between networks was calculated by distance measure, and the distance measure here was Frobenius norm [27]. The smaller the distance measure is, the higher the similarity is. And for each channel i, the formula is as follows:

$$\begin{aligned} d_{F(i)}\left(A\left(t_1\right), A\left(t_2\right)\right) &= \left\|A\left(t_1\right) - A\left(t_2\right)\right\|_{F(i)} \\ &= \sqrt{\sum_{j=1}^{N}\left(a_{ij}\left(t_1\right) - a_{ij}\left(t_2\right)\right)^2} \end{aligned} \tag{3}$$

where t represents the number of windows in DFNs, A represents the DFNs of each subject, a represents the functional network between channels, i and j are the indexes of EEG channels, and N is the total number of channels. Each channel of subject got a time-by-time graph W, which provided the necessary information to reveal the same brain state in the evolution process of dynamic brain functional network [28].

2) Recurrence Plot: According to the obtained time-by-time graph, the threshold value ϵ of the time-by-time graph W needs to be determined, which represents the upper limit of similarity between networks. When the distance measure is less than ϵ, it means that the brain functional networks corresponding to the two nodes are similar and belong to the same state, and the point of the time-by-time graph W_{ij} is set as 1. When it is greater than ϵ, the W_{ij} is set as 0, and the recurrence plot (RP) is finally obtained. By using this method, the recurrence matrix R for each subject's DFNs is given by

$$R_{i,j} = \begin{cases} 1, & W_{ij} < \varepsilon \\ 0, & W_{ij} > \varepsilon \end{cases} \tag{4}$$

where i and j represent the brain functional network at different moments. W_{ij} represents the distance measure of functional network at moment i and moment j.

3) Recurrence Quantification Analysis: Two types of recurrence quantification analysis (RQA) parameters were selected for this work [29], i.e. the recurrence rate (RR) and the trapping time (TT). RR is expressed by

$$RR = \frac{1}{N^2}\sum_{i,j=1}^{N} R_{i,j} \tag{5}$$

where N represents the total number of brain functional networks at different times. RR is used to measure the number of occurrences of particular state in RP. The higher the RR is, the more stable the network state transition is.

TT is used to estimate the average time to stay in particular state during the dynamic evolution of brain functional networks. The expression is given by

$$TT = \frac{\sum_{v=v_{\min}}^{v_{\max}} vP(v)}{\sum_{v=v_{\min}}^{v_{\max}} P(v)} \tag{6}$$

where v is the length of the vertical line in RP, and $P(v)$ is the total number of vertical lines in RP of length v, which is given by

$$P(v) = \sum_{i,j=1}^{N}\left(1 - R_{i,j-1}\right)\left(1 - R_{i,j+v}\right)\prod_{k=0}^{v-1} R_{i,j+k} \tag{7}$$

A larger TT indicates a longer time for the same state to continuously appear on the network. Based on the above method, the RR and TT of one channel are got, and the RR and TT of the whole brain are the average values of all channels.

4) Threshold Selection: In the calculation of RR and TT, different thresholds may have different effects on the results of analyzing the differences between ePD-MCI and ePD-nMCI patients. A smaller threshold may not observe the occurrence of repeated states (when the threshold value is less than 0.5, no repeated states can be observed in our work), whereas a larger threshold may cause dissimilar network states to be classified into similar states (when the threshold value is larger than 3, the network is almost always similar in our work). In the work, the threshold value was determined in the range from 1 to 3 during the construction of the RP, and the step size was increased by 0.5, and we finally determined five different thresholds. The RQA of the RP under different thresholds was carried out, and the RR and TT of the RP under the five sub-bands were obtained. In order to find the optimal threshold across all frequency bands to avoid the confusion of multiple thresholds caused by the selection of thresholds for different frequency bands, RR and TT in the five sub-bands were used as the subjects' features together. Because this paper focused on analyzing the influence of MCI on ePD patients, ePD-MCI and ePD-nMCI patients were classified by support vector machine (SVM) [30], and 5-fold cross-validation was performed. Since ten parameters (RR and TT in the five sub-bands) of 33 ePD patients were used as features, the size of the SVM input feature vector was 33 * 10. Take MCI as the label, and the size of the label was 33 * 1. We evaluated the accuracy (ACC) and area under curve (AUC) values to find the optimal threshold. The higher the value of ACC and AUC, the better the classification effect.

F. Statistical Analysis

Statistical analysis was used to quantify the between-group differences in DFNs analysis for subjects with different cognitive levels. The differences between groups were compared by the independent sample t-test. Spearman's correlation was used to evaluate the correlation between obtained parameters and MoCA scores. In order to control type I error caused by multiple comparisons due to the comparison of multiple sub-bands and electrodes, the false discovery rate (FDR) method was used to correct the statistical results. $p_{\text{FDRcorrected}} < 0.05$ indicates significant difference or significant correlation.

III. Results

Overall, the dynamic network fluctuations were significantly different in the delta, alpha, and gamma bands between ePD-MCI and ePD-nMCI patients (Fig. 2). Specifically, in the delta band, the dynamic network fluctuation in ePD-MCI patients was significantly higher than that in ePD-nMCI patients. ($t = 2.171$, $p = 0.038$ with FDR corrected). In the alpha band, the dynamic network fluctuation in ePD-nMCI patients was significantly higher than that in HC subjects ($t = 2.580$, $p = 0.037$ with FDR corrected), which

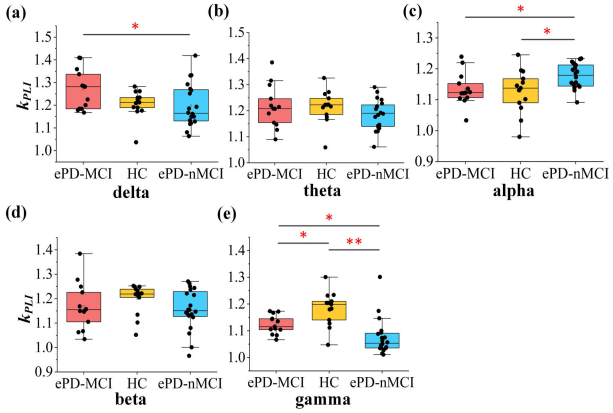

Fig. 2. Dynamic fluctuation analysis of global brain functional connectivity network in the five frequency bands (delta, theta, alpha, beta, and gamma). The analyses among ePD-MCI patients, ePD-nMCI patients, and HC were based on k_{PLI}. The p values corrected by FDR with significant differences were shown at the top of the figure in red. Asterisks (*) denoted $p < 0.05$; (**) denoted $p < 0.01$. Detailed p-values were shown in Supplementary Table III.

may be generated by PD. In addition, although there was no significant difference in the dynamic network fluctuation between HC group and ePD-MCI group, it was evident that the dynamic network fluctuation of ePD-MCI patients was markedly smaller than that of ePD-nMCI patients due to the effect of MCI (in the alpha frequency band: ePD-MCI vs. ePD-nMCI, $t = -2.572$, $p = 0.015$; ePD-MCI vs. HC, $t = 0.330$, $p = 0.930$ with FDR corrected). It indicated that MCI significantly reduced the dynamic network fluctuation in the alpha band in early PD patients. Furthermore, the opposite changes were also observed in the gamma band. The fluctuation of dynamic functional network in ePD-nMCI patients was significantly lower than that in HC ($t = -4.554$, $p < 0.001$ with FDR corrected), which indicated PD caused a significantly decrease in the dynamic network fluctuation in the gamma band. Interestingly, although the dynamic network fluctuation of ePD-MCI patients was also significantly lower than that of HC subjects, it was significantly higher than that of ePD-nMCI patients (in the gamma frequency band: ePD-MCI vs. ePD-nMCI, $t = 2.369$, $p = 0.024$; ePD-MCI vs. HC, $t = -2.912$, $p = 0.038$ with FDR corrected), which indicated that MCI significantly increases the dynamic network fluctuation in the gamma band in early PD patients.

In each frequency band, the p-value of k_{PLI} between each pair of channels was shown in Supplementary Fig. 1. In order to represent the changes more clearly in brain regions with each channel, the average k_{PLI} of one channel and the other 18 channels was compared as the k_{PLI} of this channel. As shown in Fig.3, in the left frontal, left temporal, left parietal, and occipital lobes in the delta and theta bands, the dynamic fluctuation of functional connectivity in ePD-MCI patients was apparently higher than that in ePD-nMCI patients. Importantly, in the alpha band, the dynamic fluctuation of functional connectivity in ePD-nMCI patients was considerably increased throughout the entire posterior hemisphere in comparison to HC due to the effect of PD. And the fluctuation of dFC in ePD-MCI patients was significantly

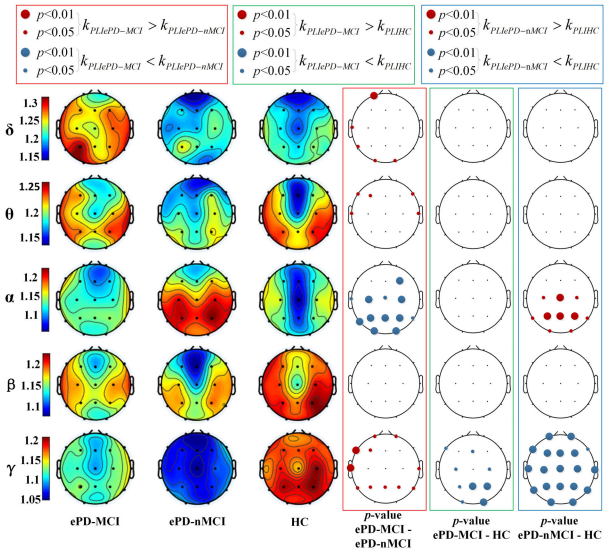

Fig. 3. The k_{PLI} analysis in each electrode in the five frequency bands. The colors in the topographic map on the left represented the average k_{PLI} parameter magnitudes at the corresponding electrodes for different groups of subjects. In each column on the right, the red point indicated that the fluctuation of dFC in the former group was significantly higher than that in the latter group, and the blue point indicated that the fluctuation of dFC in the former group was significantly lower than that in the latter group. The red box corresponded to the comparation between ePD-MCI and ePD-nMCI groups. The green box corresponded to the comparation between ePD-MCI and HC groups. The blue box corresponded to the comparation between ePD-nMCI and HC groups. The size of the point showed the different levels of significance. The large points represented $p < 0.01$, and the small points represented $p < 0.05$. For multiple comparisons, FDR correction was performed for p values. The topography map of k_{PLI} for each subject was shown in Supplementary Fig. 2.

TABLE II
THE CLASSIFICATION RESULTS UNDER THE FIVE THRESHOLDS BASED ON SVM BETWEEN EPD-MCI AND EPD-NMCI GROUPS

Threshold	ACC mean(s.d.)	AUC mean(s.d.)
Distance = 1	0.8524(0.1016)	0.9222(0.1083)
Distance = 1.5	0.8476(0.1019)	0.9133(0.1445)
Distance = 2	0.8048(0.2748)	0.8556(0.2208)
Distance = 2.5	0.8238(0.1558)	0.8600(0.1422)
Distance = 3	0.8143(0.1308)	0.8883(0.0904)

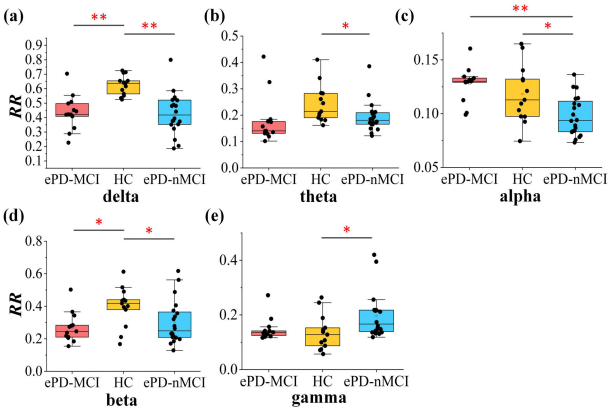

Fig. 4. Analysis of whole-brain RR in the five frequency bands. The analyses among ePD-MCI patients, ePD-nMCI patients, and HC subjects were based on RR. The p values corrected by FDR with significant differences were shown at the top of the figure in red. Asterisks (*) denoted $p < 0.05$; (**) denoted $p < 0.01$. Detailed p-values were shown in Supplementary Table IV.

lower than that in ePD-nMCI patients in the central region, parietal, occipital, right frontal, and left temporal lobes in the alpha band, which might be generated by MCI. By the effect of PD and MCI, there was no significant difference between ePD-MCI patients and HC. Moreover, in the gamma band, the dynamic fluctuation of functional connectivity in ePD-nMCI patients was markedly lower than HC subjects in all regions due to PD. The fluctuation of dFC in left frontal, temporal, and parietal lobes of ePD-MCI patients in the gamma band was significantly higher than that in ePD-nMCI patients. Based on that, there were less significant differences in left frontal and temporal lobes between ePD-MCI patients and HC subjects. Through the analysis of the fluctuation of dFC in the whole brain and different brain regions, it was found that the dynamic fluctuations of functional connectivity in early PD were generally increased in delta and gamma bands, which was induced by MCI, and these changes mainly occurred in the left frontal, temporal, and parietal lobes. Whereas the fluctuation of dFC in early PD without MCI were obviously decreased in the central, parietal, occipital, right frontal, and left temporal lobes in the alpha band.

When analyzing the state transition of DFNs, it was necessary to determine the threshold value to construct the RP by time-by-time graph. We used SVM to calculate ACC and AUC between ePD-MCI and ePD-nMCI groups, and combined a total of 10 parameters of RR and TT in five frequency bands in each patient into a feature vector as the input of SVM under each threshold. The size of the input feature vector was 33*10. The mean and standard deviation of ACC and AUC between ePD-MCI and ePD-nMCI groups under different thresholds were shown in Table II. From the classification results, we found that ACC and AUC under threshold 1 were generally higher than other conditions. It meant that there was a greater difference in RR and TT between ePD-MCI and ePD-nMCI patients when the threshold was 1. Therefore, the threshold value of 1 was selected to construct the RP.

RR and TT of the whole brain in different frequency bands were obtained according to the RP. As a whole, the RR values in ePD-MCI patients were significantly higher than those in ePD-nMCI patients (Fig. 4). In the delta and beta bands, it was found that the RR in both ePD-MCI and ePD-nMCI patients was significantly lower than that of HC (in the delta frequency band: ePD-MCI vs. HC, $t = -4.905$, $p < 0.001$; ePD-nMCI vs. HC, $t = -5.282$, $p < 0.001$; in the beta frequency band: ePD-MCI vs. HC, $t = -3.035$, $p < 0.014$; ePD-nMCI vs. HC, $t = -2.129$, $p = 0.041$ with FDR corrected). Additionally, when compared with HC, the RR in ePD-nMCI patients was significantly lower in the theta band ($t = -2.184$, $p = 0.041$ with FDR corrected) and higher in the gamma band ($t = 2.287$, $p = 0.041$ with FDR corrected). Interestingly, there was no discernible difference between ePD-MCI and ePD-nMCI patients in the above four bands (in the delta frequency band: $t = 0.156$, $p = 0.877$; in the theta frequency band: $t = -0.540$, $p = 0.593$; in the beta frequency band: $t = -0.728$, $p = 0.472$; in the gamma frequency band:

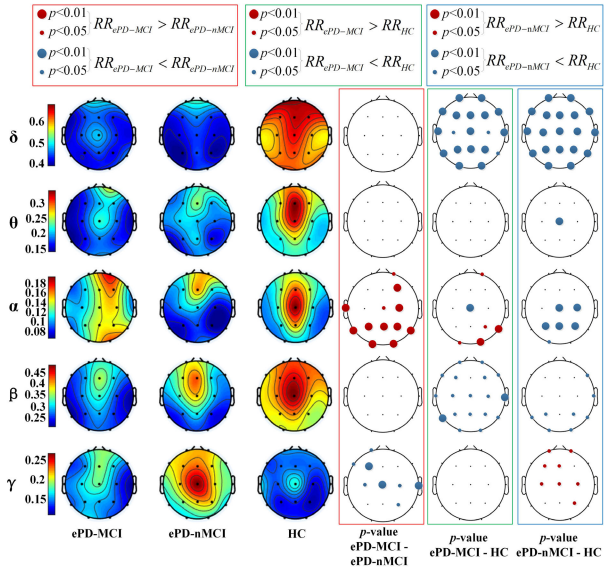

Fig. 5. The *RR* analysis in each electrode in the five frequency bands. The analyses among ePD-MCI patients, ePD-nMCI patients, and HC subjects were based on *RR*. The colors in the topographic map on the left represented the average *RR* parameter magnitudes at the corresponding electrodes for different groups of subjects. In each column on the right, the red points represented the positions in which the *RR* of DFNs in the former group was significantly higher than that in the latter group. And the blue points represented the positions in which the *RR* of DFNs in the former group was significantly lower than that in the latter group. The red box corresponded to the comparation between ePD-MCI and ePD-nMCI groups. The green box corresponded to the comparation between ePD-MCI and HC goups. The blue box corresponded to the comparation between ePD-nMCI and HC groups. The size of the point showed the different levels of significance. The large points represented $p < 0.01$, and the small points represented $p < 0.05$. For multiple comparisons, FDR correction was performed for *p* values. The topography map of *RR* for each subject was shown in Supplementary Fig. 3.

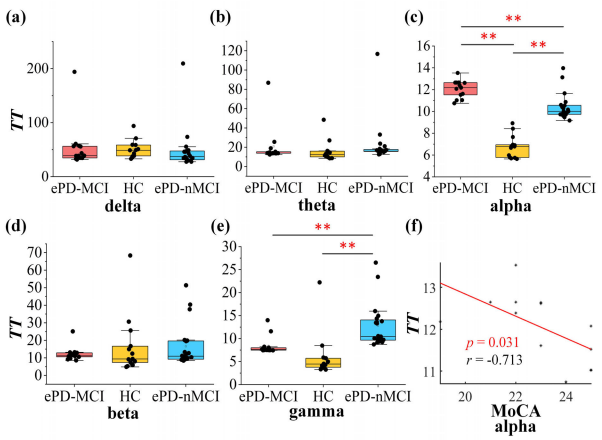

Fig. 6. The analysis of whole-brain *TT* in the five frequency bands. (a)-(e) The analyses of differences among ePD-MCI patients, ePD-nMCI patients, and HC were based on *TT*. The *p* values corrected by FDR with significant differences were shown at the top of the figure in red. Asterisks (*) denoted $p < 0.05$; (**) denoted $p < 0.01$. Detailed *p*-values were shown in Supplementary Table V. (f) Spearmans correlation analysis between *TT* values and MoCA scores of ePD-MCI patients in the alpha band. For multiple comparisons, FDR correction is performed for *p* values. And the results with significant differences were highlighted in red.

$t = -2.002$, $p = 0.054$ with FDR corrected). It indicates that PD causes the above-mentioned decrease of RR in delta, theta, and beta bands, and the increase of RR in the theta band. It was worth noting that in the alpha band, the RR in ePD-nMCI patients was much lower than HC due to the effect of PD ($t = -2.606$, $p = 0.035$ with FDR corrected). Whereas the RR in ePD-MCI patients in the alpha band was significantly greater than patients with ePD-nMCI ($t = 4.800$, $p < 0.001$ with FDR corrected), and it was not significantly different from that in HC ($t = 1.096$, $p = 0.355$ with FDR corrected), which suggested that MCI significantly decreased the network transition stability in the alpha band in early PD patients.

We found that there were significant differences in RR of the whole brain network states between ePD-MCI and ePD-nMCI patients in the alpha band. There were significant differences between ePD-MCI and ePD-nMCI patients in alpha and gamma bands (Fig. 5). It was found that in the alpha band, RR significantly decreased in ePD-nMCI patients in the central region and parietal lobe compared with HC, whereas the RR considerably increased in the right frontal, left temporal, central, parietal, and occipital lobes in ePD-MCI compared with ePD-nMCI patients, making the RR in ePD-MCI patients considerably higher in right parietal and occipital lobes than that in HC. It suggested that the network transition stability in early PD was abnormally increased in the right frontal, left temporal, central, parietal, and occipital lobes in the alpha band by the effect of MCI. Although there was no significant difference in RR in the whole brain between ePD-MCI and ePD-nMCI patients in the gamma band, the RR in the left frontal, central, and right temporal lobes in the gamma band in ePD-MCI patients was significantly lower than that in ePD-nMCI patients. Additionally, associated with the increase in RR between ePD-nMCI patients and HC in the frontal and central regions in the gamma band generated by PD, there was no significant difference between ePD-MCI patients and HC subjects. It indicates that in the gamma band, MCI leads to the aberrant decrease in network transition stability in frontal and central regions in early PD patients.

As shown in Fig. 6, the TT between ePD-MCI and ePD-nMCI patients varied widely in alpha and gamma bands. Specifically, in the alpha band, the TT of the whole brain in ePD-nMCI patients was considerably higher than that in HC ($t = 8.917$, $p < 0.001$ with FDR corrected), caused by the effects of PD. In addition, the TT in ePD-MCI patients was noticeably higher than ePD-nMCI patients in the alpha band ($t = 4.251$, $p < 0.001$ with FDR corrected), and obviously, it was also significantly higher than that in HC ($t = 14.331$, $p < 0.001$ with FDR corrected), which might be generated by MCI. In the gamma band, the TT in ePD-nMCI patients was significantly higher than that in HC due to the effect of PD ($t = 3.887$, $p = 0.001$ with FDR corrected). And there was no significant difference between HC subjects and ePD-MCI patients ($t = 1.577$, $p = 0.320$ with FDR corrected) based on the ePD-MCI patients' considerably lower TT in the gamma band compared to ePD-nMCI patients ($t = -3.641$, $p = 0.004$ with FDR corrected). It indicated that the duration of network state was abnormally increased in the alpha band

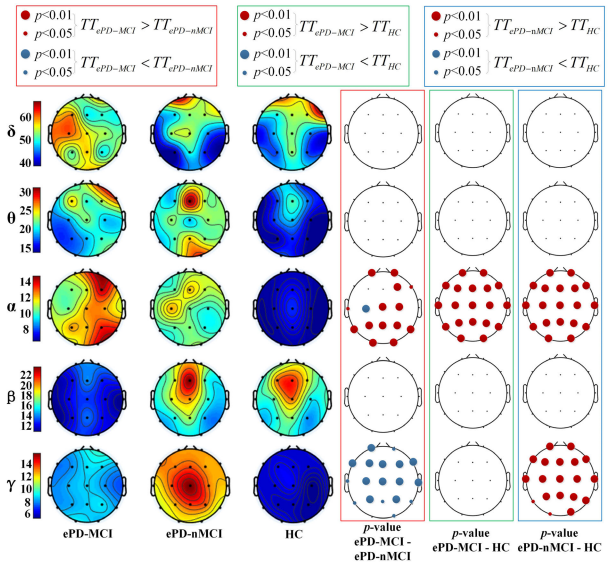

Fig. 7. The analysis of TT in each electrode in the five frequency bands. The colors in the topographic map on the left represented the average TT parameter magnitudes at the corresponding electrodes for different groups of subjects. In each column on the right, the red points represented the positions in which the TT of DFNs in the former group was significantly higher than that in the latter group. And the blue points represented the positions in which the TT of DFNs in the former group was significantly lower than that in the latter group. The red box corresponded to the comparation between ePD-MCI and ePD-nMCI groups. The green box corresponded to the comparation between ePD-MCI and HC groups. The blue box corresponded to the comparation between ePD-nMCI and HC groups. The size of the point showed the different levels of significance. The large points represented $p < 0.01$, and the small points represented $p < 0.05$. For multiple comparisons, FDR correction was performed for p values. The topography map of TT for each subject was shown in Supplementary Fig. 4.

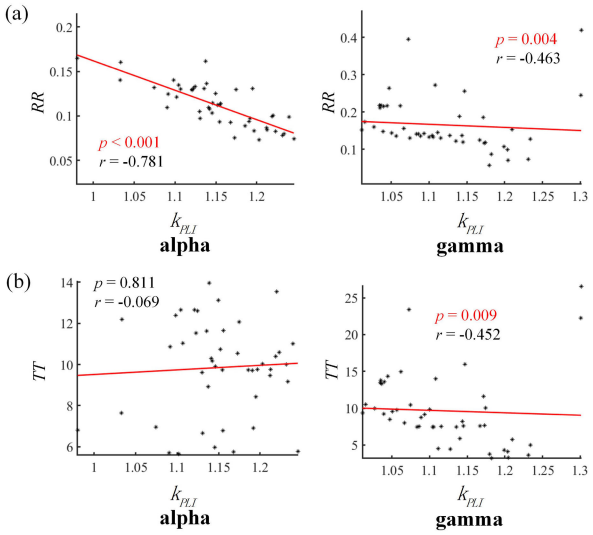

Fig. 8. (a) Spearmans correlation analysis between RR and k_{PLI} in alpha and gamma bands. (b) Spearmans correlation analysis between TT and k_{PLI} in alpha and gamma bands. FDR correction was performed for p values, and the results with significant differences were highlighted in red.

and abnormally decreased in the gamma band in early PD patients by MCI. For correlation analysis, in the alpha band, we observed that the TT of ePD-MCI patients was negatively correlated with the MoCA scale scores ($r = -0.713$, $p = 0.031$ with FDR corrected).

As shown in Fig.7, in the alpha band, we discovered that the TT in ePD-nMCI patients was considerably higher than that in HC throughout the whole brain regions due to the effect of PD. With the significant increase in TT in ePD-MCI patients in the frontal, parietal, central, and occipital lobes, ePD-MCI patients TT was considerably higher than HC in the whole brain in the alpha band. Similarly, ePD-nMCI patients showed a statistically significant increase in TT throughout these regions when compared to HC in the gamma band. In contrast to the alpha band, there was no significant differences between ePD-MCI patients and HC in the gamma band, while the significant decreases in TT were existed in ePD-MCI patients compared to ePD-nMCI patients in the almost whole brain. It was represented that according to the network state duration in early PD patients, MCI caused the significant increase in the frontal, parietal, central, and occipital lobes in the alpha band, and the significant decrease in the whole brain in the gamma band.

In the analysis of fluctuation about dFC, it was found that the fluctuation in the central, parietal, occipital, right frontal, and left temporal lobes in ePD-MCI patients was significantly lower than that in ePD-nMCI patients in the alpha band, and the fluctuation in left frontal, temporal, and parietal lobes of ePD-MCI patients in the gamma band was significantly higher than in ePD-nMCI patients. This was consistent with the stability analysis of network state transition, so it was suspected that the stability of network state transition might be caused by the fluctuation of dFC. Therefore, Spearman's correlation analysis was conducted respectively for whole-brain RR, TT, and k_{PLI} of all participants (all PD patients and HC subjects) in alpha and gamma bands, as shown in Fig. 8. RR and k_{PLI} had significant negative correlation in both alpha and gamma bands, indicating that the increased fluctuation of dFC leads to more frequent internal DFNs switching. The correlation between RR and k_{PLI} indicated that the fluctuation of functional connections affected the stability of network state transition. However, there was no correlation between TT and k_{PLI} in the alpha band. The analysis results indicated that the fluctuation of dFC might lead to frequent network state switching, but did not affect the duration of state switching.

IV. Discussion

To explore the specificity of brain network in ePD-MCI patients, a comparative work was carried out in this work in ePD-MCI, ePD-nMCI, and HC groups. By constructing the DFNs using EEG data, the fluctuations and state transition of dFC were analyzed. The main results of this paper were summarized in Supplementary Fig. 5.The results showed that, the abnormal fluctuation of dFC between ePD-MCI and ePD-nMCI was related to rhythm, and the abnormal fluctuation of dFC was a process from significant rise to significant fall and then to significant rise with the increase of the rhythm in the five sub-bands. In our work, it was found that the excessively stable and hyperactive states were abnormal phenomena of the ePD functional network affected by MCI in different rhythms, which may affect the effective

information integration of different functional brain regions. Based on the correlation between RR and k_{PLI}, it was found that the increase in the fluctuation of dFC between regions corresponded to the decrease in the stability of the dynamic network, and similarly, the decrease in the dynamic fluctuation corresponds to the increase in the stability of the network. There was significant negative correlation between k_{PLI} and RR in the alpha band and gamma band, indicating that the fluctuation of dFC affected the DFNs stability.

In comparison to HC, it was shown that ePD-nMCI patients had higher k_{PLI} and lower RR in the alpha band. Conti et al. [21] found that some cortical regions of early PD patients began to establish or increase connectivity with other regions in the alpha band to make up for the defects caused by PD, which accorded with our findings that the fluctuation of dFCs of ePD-nMCI patients was higher than that of HC in the alpha band. Evangelisti et al. [31] found that the posterior cingulate was the primary driving region of the functional connectivity of early PD patients in the alpha band. The abnormal drives in brain might lead to our findings of increased fluctuation of dFCs in the whole posterior hemisphere of ePD-nMCI patients in the alpha band. Li et al. [32] discovered that the clustering coefficient and local efficiency of the EEG-based brain network in the alpha band in PD patients were significantly reduced, suggesting that their brain networks were more fragile and unstable than those of HC. On the other hand, it was reported that PD patients gamma band efficiency had increased overall [21]. It was consistent with the opposite findings, which showed that ePD-nMCI patients had higher RR and lower k_{PLI} in the gamma band when compared to HC subjects. Moreover, the TT of ePD-nMCI patients was increased significantly in both alpha and gamma bands, which is consistent with studies that the EEG of PD patients slows down, especially in the alpha band [33].

Based on the differences between ePD patients and healthy controls, we paid close attention to the significant changes between ePD-MCI and ePD-nMCI patients. In the alpha band, the fluctuation of dFC decreased in the right frontal, left temporal, parietal, central, and occipital lobes, and the stability of network transition and duration of network state increased in those regions in ePD-MCI group. They might be caused by cognitive impairment affecting ePD patients, and might serve as the potential physiological marker. The decrease in alpha rhythm and alpha band energy in the brains affected by cognitive impairment might be the reason for the overall decrease in functional connectivity fluctuations and the increase in network transition stability in the alpha band in ePD-MCI patients. It was discovered that the functional connectivity of alpha band in PD patients was gradually decreased and interrupted with the deterioration of cognitive ability [34]. According to sen Bhattacharya et al. [35], Alzheimer's disease (AD) caused the brain's alpha rhythms to slow down and its alpha band power to decline. In the process of decreasing alpha power, the brain maintained the stability of alpha band by local compensation [36], which might lead to the increase in network transition stability. Decrease in alpha rhythm activity was also identified as one of the biomarkers to distinguish PD patients with normal cognition from PD with MCI [37]. The decreased state transition and increased state residence time that we found were associated with PDD [38]. Furthermore, we found the abnormally increased fluctuation of dFC in the gamma band. van Deursen et al. [39] suggested that the increased gamma-band rhythm in AD patients may be the reason for the excessive activation of the brain network. Additionally, they found an increase in the coupling strength between the gamma and the low-frequency bands in frontal and parietal regions, suggesting a reduction in the brain network complexity. This is consistent with our finding. In addition, we found that the functional network of ePD-MCI patients in the gamma band was in non-stationary mode, which was specifically manifested in the decline of network transition stability and network state duration. These changes in ePD-MCI may be due to the brain overcompensating for the functional defects, which leads to the damage of inhibitory neurons, thus causing the excessive neuron activity at high frequency bands [40] to produce the dynamic non-stationary of the network. Similarly, the over coupling found in the gamma band of AD patients indicated that the network complexity was weakened, which meant that more neural resources need to be used [39]. Excessive local neuronal activity has been shown to increase amyloid-Â deposition [41]. The neuropathological mechanism analysis of the cognitive impairment in PD suggests that the decrease in cognitive function in PD may be related to the occurrence of pathological amyloid-β [42]. Taken together, these discussions explain that MCI can lead to abnormal changes in the dynamic characteristics of brain functional connectivity network in alpha and gamma frequency bands in early PD patients.

In our selected subjects, we did not find a significant difference in age between ePD-MCI patients and ePD-nMCI patients, ruling out a potential confounding effect of age on the results of the analysis. There were also some limitations in this paper. The assessment of subjects' cognitive degree was only based on MOCA, and more detailed neuropsychological assessment was lacking. Whether the results of our study can be used as a diagnostic test basis for PD-MCI population, the external validity still requires in-depth cooperation with hospitals to obtain new data and conduct repeated tests to verify it.

V. Conclusion

We revealed the characteristics of dynamic brain functional network in ePD-MCI. The fluctuation of the dFC and the stability of state transition based on DFNs in each EEG frequency band were calculated to evaluate the state changes of different brain regions in ePD-MCI patients. In the alpha band of EEG, we observed that compared with ePD-nMCI group, the k_{PLI} of patients with ePD-MCI was significantly decreased in the right frontal, left temporal, central, parietal, and occipital lobe, while RR and TT were significantly increased in these regions. It indicated that in ePD-MCI patients, the dynamic connectivity fluctuation of those regions was abnormally decreased and the stability of functional connectivity networks was abnormally increased in EEGs alpha band. In contrast, in the gamma band of EEG, the k_{PLI} was significantly increased

and the TT was significantly decreased in ePD-MCI patients, which suggested that the functional network in ePD-MCI patients was found to be in a non-stationary mode. The regions of the brain with abnormally increased fluctuation of dynamic connectivity mainly concentrated on the left frontal, temporal, and parietal lobes. And the stability of functional network was decreased in the central, left frontal, and right temporal lobes. The aberrant duration of network state in ePD-MCI patients in the alpha band was significantly negatively correlated with cognitive function ($r = -0.713$, $p = 0.031$ with FDR corrected), which might pave the way to identify and predict cognitive impairment in early PD patients.

REFERENCES

[1] A. Lee and R. M. Gilbert, "Epidemiology of Parkinson disease," *Neurologic Clinics*, vol. 34, no. 4, pp. 955–965, Nov. 2016.

[2] R. B. Postuma et al., "MDS clinical diagnostic criteria for Parkinson's disease," *Movement Disorders*, vol. 30, no. 12, pp. 1591–1601, Oct. 2015.

[3] D. Muslimovic, B. Post, J. D. Speelman, and B. Schmand, "Cognitive profile of patients with newly diagnosed Parkinson disease," *Neurology*, vol. 65, no. 8, pp. 1239–1245, Oct. 2005.

[4] D. Aarsland et al., "Cognitive decline in Parkinson disease," *Nature Rev. Neurol.*, vol. 13, no. 4, pp. 217–231, Mar. 2017.

[5] A. Q. Rana, M. S. Yousuf, S. Naz, and N. Qa'aty, "Prevalence and relation of dementia to various factors in Parkinson's disease," *Psychiatry Clin. Neurosciences*, vol. 66, no. 1, pp. 64–68, Feb. 2012.

[6] L. Schneider, V. Seeger, L. Timmermann, and E. Florin, "Electrophysiological resting state networks of predominantly akinetic-rigid Parkinson patients: Effects of dopamine therapy," *NeuroImage, Clin.*, vol. 25, 2020, Art. no. 102147.

[7] R. Yuvaraj, "Emotion processing in Parkinson's disease: An EEG spectral power study," *Int. J. Neurosci.*, vol. 124, no. 7, pp. 491–502, Jul. 2014.

[8] M. Chaturvedi et al., "Phase lag index and spectral power as QEEG features for identification of patients with mild cognitive impairment in Parkinson's disease," *Clin. Neurophysiol.*, vol. 130, no. 10, pp. 1937–1944, Oct. 2019.

[9] H. Bousleiman et al., "Power spectra for screening parkinsonian patients for mild cognitive impairment," *Ann. Clin. Translational Neurol.*, vol. 1, no. 11, pp. 884–890, Nov. 2014.

[10] S. Galantucci et al., "Structural brain connectome and cognitive impairment in Parkinson's disease," *Radiology*, vol. 283, no. 2, pp. 515–525, May 2017.

[11] O. Bezdicek et al., "Mild cognitive impairment disrupts attention network connectivity in Parkinson's disease: A combined multimodal MRI and meta-analytical study," *Neuropsychologia*, vol. 112, pp. 105–115, Apr. 2018.

[12] M. Rubinov and O. Sporns, "Complex network measures of brain connectivity: Uses and interpretations," *NeuroImage*, vol. 52, no. 3, pp. 1059–1069, Sep. 2010.

[13] A. A. P. Suárez, S. B. Batista, I. P. Ibáñez, E. C. Fernández, M. F. Campos, and L. M. Chacón, "EEG-derived functional connectivity patterns associated with mild cognitive impairment in Parkinson's disease," *Behav. Sci.*, vol. 11, no. 3, p. 40, Mar. 2021.

[14] R. Hindriks et al., "Can sliding-window correlations reveal dynamic functional connectivity in resting-state fMRI?" *NeuroImage*, vol. 127, pp. 242–256, Feb. 2016.

[15] M. D. Fox and M. E. Raichle, "Spontaneous fluctuations in brain activity observed with functional magnetic resonance imaging," *Nature Rev. Neurosci.*, vol. 8, no. 9, pp. 700–711, Sep. 2007.

[16] E. Tognoli and J. A. S. Kelso, "The metastable brain," *Neuron*, vol. 81, no. 1, pp. 35–48, Jan. 2014.

[17] Q. Long et al., "Graph-theoretical analysis identifies transient spatial states of resting-state dynamic functional network connectivity and reveals dysconnectivity in schizophrenia," *J. Neurosci. Methods*, vol. 350, pp. 1–11, Feb. 2021.

[18] M. Díez-Cirarda et al., "Dynamic functional connectivity in Parkinson's disease patients with mild cognitive impairment and normal cognition," *NeuroImage, Clin.*, vol. 17, pp. 847–855, Dec. 2017.

[19] K. K. Tan, H. Dou, Y. Chen, and T. H. Lee, "High precision linear motor control via relay-tuning and iterative learning based on zero-phase filtering," *IEEE Trans. Control Syst. Technol.*, vol. 9, no. 2, pp. 244–253, Mar. 2001.

[20] E. Oja and Z. Yuan, "The FastICA algorithm revisited: Convergence analysis," *IEEE Trans. Neural Netw.*, vol. 17, no. 6, pp. 1370–1381, Nov. 2006.

[21] M. Conti et al., "Brain functional connectivity in de novo Parkinson's disease patients based on clinical EEG," *Frontiers Neurol.*, vol. 13, pp. 1–9, Mar. 2022.

[22] X. Chen, Z. Wu, and N. E. Huang, "The time-dependent intrinsic correlation based on the empirical mode decomposition," *Adv. Adapt. Data Anal.*, vol. 2, no. 2, pp. 233–265, Apr. 2010.

[23] X. Zhuang et al., "Single-scale time-dependent window-sizes in sliding-window dynamic functional connectivity analysis: A validation study," *NeuroImage*, vol. 220, Oct. 2020, Art. no. 117111.

[24] C. J. Stam, G. Nolte, and A. Daffertshofer, "Phase lag index: Assessment of functional connectivity from multi channel EEG and MEG with diminished bias from common sources," *Hum. Brain Mapping.*, vol. 28, no. 11, pp. 1178–1193, Nov. 2007.

[25] D. Kugiumtzis, "Surrogate data test on time series," *Model. Forecasting Financial Data*, vol. 2, pp. 267–282, Nov. 2002.

[26] J. D. Medaglia et al., "Flexible traversal through diverse brain states underlies executive function in normative neurodevelopment," *Quant. Biol.*, pp. 1–14, Oct. 2015, doi: 10.48550/arXiv.1510.08780.

[27] A. Kurmukov, Y. Dodonova, and L. Zhukov, "Classification of normal and pathological brain networks based on similarity in graph partitions," in *Proc. IEEE 16th Int. Conf. Data Mining Workshops (ICDMW)*, Dec. 2016, pp. 107–112.

[28] R. Chen et al., "Task-related multivariate activation states during task-free rest," *bioRxiv*, Apr. 2017, doi: 10.1101/068221.

[29] N. Marwan, M. C. Romano, M. Thiel, and J. Kurths, "Recurrence plots for the analysis of complex systems," *Phys. Rep.*, vol. 438, nos. 5–7, pp. 237–329, 2007.

[30] S. Cuentas, R. Peñabaena-Niebles, and E. Garcia, "Support vector machine in statistical process monitoring: A methodological and analytical review," *Int. J. Adv. Manuf. Technol.*, vol. 91, nos. 1–4, pp. 485–500, Jul. 2017.

[31] S. Evangelisti et al., "L-dopa modulation of brain connectivity in Parkinson's disease patients: A pilot EEG-fMRI study," *Frontiers Neurosci.*, vol. 13, p. 611, Jun. 2019.

[32] Z. Li et al., "Abnormal functional brain network in Parkinson's disease and the effect of acute deep brain stimulation," *Frontiers Neurol.*, vol. 12, Oct. 2021, Art. no. 715455.

[33] R. C. Rea et al., "Quantitative EEG and cholinergic basal forebrain atrophy in Parkinson's disease and mild cognitive impairment," *Neurobiol. Aging*, vol. 106, pp. 37–44, Oct. 2021.

[34] M. Hassan et al., "Functional connectivity disruptions correlate with cognitive phenotypes in Parkinson's disease," *NeuroImage, Clin.*, vol. 14, pp. 591–601, Mar. 2017.

[35] B. S. Bhattacharya, D. Coyle, and L. P. Maguire, "A thalamo–cortico–thalamic neural mass model to study alpha rhythms in Alzheimer's disease," *Neural Netw.*, vol. 24, no. 6, pp. 631–645, Aug. 2011.

[36] K. Abuhassan, D. Coyle, and L. Maguire, "Compensating for thalamocortical synaptic loss in Alzheimer's disease," *Frontiers Comput. Neurosci.*, vol. 8, no. 65, pp. 1–18, Jun. 2014.

[37] V. V. Cozac, U. Gschwandtner, F. Hatz, M. Hardmeier, S. Rüegg, and P. Fuhr, "Quantitative EEG and cognitive decline in Parkinson's disease," *Parkinson's Disease*, vol. 2016, pp. 1–14, Apr. 2016.

[38] E. Fiorenzato et al., "Dynamic functional connectivity changes associated with dementia in Parkinson's disease," *Brain*, vol. 142, no. 9, pp. 2860–2872, Sep. 2019.

[39] J. A. van Deursen, E. F. P. M. Vuurman, F. R. J. Verhey, V. H. J. M. van Kranen-Mastenbroek, and W. J. Riedel, "Increased EEG gamma band activity in Alzheimer's disease and mild cognitive impairment," *J. Neural Transmiss.*, vol. 115, no. 9, pp. 1301–1311, Sep. 2008.

[40] M. J. Hogan, G. R. J. Swanwick, J. Kaiser, M. Rowan, and B. Lawlor, "Memory-related EEG power and coherence reductions in mild Alzheimer's disease," *Int. J. Psychophysiology*, vol. 49, no. 2, pp. 147–163, Aug. 2003.

[41] W. de Haan, K. Mott, E. C. W. van Straaten, P. Scheltens, and C. J. Stam, "Activity dependent degeneration explains hub vulnerability in Alzheimer's disease," *PLoS Comput. Biol.*, vol. 8, no. 8, Aug. 2012, Art. no. e1002582.

[42] E. N. Wilson et al., "Soluble TREM2 is elevated in Parkinson's disease subgroups with increased CSF tau," *Brain*, vol. 143, no. 3, pp. 932–943, Mar. 2020.